Journal of Fluorescence, Vol. 6, No. 4, 1996

Dynamics of *Lens culinaris* Agglutinin Studied by Red-Edge Excitation Spectra and Anisotropy Measurements of 2-*p*-Toluidinylnaphthalene-6-Sulfonate (TNS) and of Tryptophan Residues

J. R. Albani[1]

Received October 6, 1995; accepted September 16, 1996

The fluorescence of 2-p-toluidinylnaphthalene-6-sulfonate bound to *Lens culinaris* agglutinin and of the Trp residues of the protein was investigated. Red-edge excitation spectra and steady-state anisotropy as a function of temperature indicate that the TNS is bound rigidly. Red-edge excitation spectra, steady-state anisotropy as a function of sucrose and anisotropy decay experiments performed on Trp residues fluorescence prove that the internal fluorophore presents residual motion independent of the global rotation of the protein. Fluorescence anisotropy decay allows to calculate the rotational correlation time (351 ps) of this local motion. Quenching resolved emission anisotropy with iodide gives values equal to 0.257 and 0.112 for the anisotropies of the buried and the surface Trp residues, respectively. This result indicates that the Trp residues present at the surface of the protein have important local motions compared to those embedded in the protein matrix. The results obtained from TNS and Trp residues indicate that the agglutinin has different dynamic domains.

KEY WORDS: *Lens culinaris* agglutinin; 2-*p*-toluidinylnaphthalene-6-sulfonate; tryptophan; red-edge excitation shift; steady-state anisotropy; fluorescence anisotropy decay; quenching resolved emission anisotropy; protein dynamics.

INTRODUCTION

Lectins are proteins capable of recognizing and binding specific carbohydrate structures.[1,2] They play an important role in immunology and hematology and are used as specific probes for membrane glycoprotein structures. Legume lectins have an important role in seed maturation, cell wall assembly, and the defense mechanism.

Composed of two α and two β chains (MW = 5710[3–5] and 20,572,[5] respectively), the lentil lectin, *Lens culinaris* agglutinin (LCA), is a tetramer $\alpha_2\beta_2$ with a molecular weight equal to 52,570.[5] LCA contains five Trp residues, three embedded in the protein matrix, and two near the protein surface. Trp 53β is the most accessible to the protein surface, followed by Trp 128β. Trp 152β, Trp 19α, and Trp 40α are buried in the protein core. Trp 19α is completely buried, with zero accessibility to the water surrounding the surface of the protein (R. Loris, personal communication).

The fluorescence of intrinsic fluorophores such as Trp residues and/or extrinsic ones such as toluidinylnaphthalene-6-sulfonate (TNS) are used to study the motion of proteins. Dynamics of proteins are investigated by fluorescence anisotropy decay, steady-state measurements of emission anisotropy, and red-edge excitation

[1] Laboratoire de Biophysique Moléculaire, Université des Sciences et Technologies de Lille, B.P. 649, 59656 Villeneuve d'Ascq Cédex, France.

1053-0509/96/1200-0199$09.50/0

shift experiments.[6–11] In a protein such as LCA, when Trp residues are used as a probe, the local motion measured by the previous methods concerns both classes of Trp residues and thus represents an average measure of dynamics. The exposed tryptophans would be expected to rotate much more freely than the buried residues. This will heavily weight the average rotation observed and will reduce the sensitivity of the quantitative determination of the rotation of the buried residues. In order to study the dynamic behavior of each class of tryptophanyl residues, steady-state measurements of emission anisotropy under conditions of selective quenching can be carried out.[12]

In this work, red-edge excitation shift, steady-state anisotropy as a function of sucrose, fluorescence anisotropy decay, and quenching resolved emission anisotropy are applied to the Trp residues of LCA. Our results indicate that the Trp residues of the protein surface have important residual motions independent of the global rotation of the protein, while those embedded in the protein matrix are much less mobile.

TNS binds to LCA with a stoichiometry of 1:1 and a dissociation constant of 8 μM.[13] Red-edge excitation and steady-state fluorescence anisotropy measurements, as a function of temperature, of TNS bound to the LCA indicate that the fluorescent probe is bound rigidly to a hydrophobic site. Results obtained from Trp residues and TNS clearly show that LCA has different dynamic domains.

MATERIALS AND METHODS

Lens culinaris agglutinin was isolated and purified as described in Refs. 14 and 15. The lyophilized protein was dissolved in a 10 mM phosphate, 0.143 M NaCl buffer, pH 7. Its concentration was determined spectrophotometrically at 280 nm ($E^{1\%}_{1\,cm}$ = 12.5).[16] In red-edge excitation shift and in fluorescence quenching studies, the concentration of the lectin was equal to 5 μM. In steady-state anisotropy measurements and in fluorescence anisotropy decay, the protein concentration was equal to 10 μM.

The concentration of TNS (from Sigma) was determined spectrophotometrically using an extinction coefficient equal to 18.9 mM^{-1} cm^{-1} at 317 nm.[17]

KI was from Sigma. To the stock solution (4 M), $Na_2S_2O_3$ (10^{-2} M) was added to avoid the formation of I_3^-.

Sucrose was from Janssen (Beerse, Belgium). A solution of 60% sucrose was prepared by dissolving 10 g of sucrose in 10 ml of buffer. Heating accelerates and facilitates obtaining a homogeneous solution. Once the sucrose dissolved, we added buffer to reach a final volume of 20 ml.

Absorbance data were obtained with a Shimadzu MPS-2000 spectrophotometer using 1-cm-pathlength cuvettes.

Fluorescence spectra were obtained with a Perkin–Elmer LS-5B spectrofluorometer. Bandwidths used for excitation and emission were 2.5 and 5 nm for studies with Trp residues and TNS, respectively.

The quartz cuvettes had optical pathlengths equal to 1 and 0.4 cm for the emission and excitation wavelengths, respectively. The observed fluorescence intensities were first corrected for dilution, and then corrections were made for absorption by the following formula:[18]

$$F_{corr} = F_{obs}\ \text{antilog}[OD_{cx} + OD_{em}]/2 \qquad (1)$$

where F_{obs} is the intensity corrected for dilution, F_{corr} is the intensity after correction for absorption, and OD_{ex} and OD_{em} are the optical densities at the excitation and emission wavelengths, respectively. Finally, fluorescence spectra were corrected for the Raman effect of the buffer and for the fluorescence of free TNS in solution.

Steady-state anisotropy was measured with the same Perkin–Elmer fluorometer used for the emission spectra acquisition. Bandwidths used for excitation and emission were both 5 and 10 nm for experiments measuring Trp and TNS fluorescence, respectively.

Fluorescence lifetimes and fluorescence anisotropy decay were obtained by the time-correlated single-photon counting technique from the polarized components VV and VH on the experimental setup installed on the SB_1, window of the Synchrotron Radiation machine super-ACO (Anneau de collision d'Orsay), which is described in Ref. 19. The storage ring provides a light pulse with a full width at half maximum of about 500 ps at a frequency of 8.33 MHz for a double-bunch mode. The excitation and emission bandwidths were set at 5 and 10 nm, respectively. In most experiments a Hammamatsu microchannel plate R1564U-06 was utilized. Data for $I_{vv}(t)$ and $I_{vh}(t)$ were stored in separate memories of a plug-in multichannel analyzer card (Canberra) in a DESKPRO 286E microcomputer (Compaq). Accumulation was stopped when 10^5 counts was stored in the peak channel for the total fluorescence intensity decay. The instrument response function was automatically monitored in alternation with the parallel and perpendicular components of the polarized fluorescence decay by measuring the sample-scattering light at the emission wavelength. The automatic sampling of the data was driven by the microcomputer.[20,21] In the time correlated

single photon counting, the detection system measures the time between the excited pulse and the arrival of the first photon. The distribution of arrival times represents the decay curve.

Analysis of the fluorescence intensity decay data as a sum of 150 exponentials was performed by the Maximum Entropy Method (MEM)[22] using the commercially available library of subroutines MEMSYS 5 (MEDC Ltd., UK) as a library of subroutines.

With vertically polarized light, the parallel $I_{vv}(t)$ and perpendicular $I_{vh}(t)$ components of the fluorescence intensity at time t after the start of the excitation are

$$I_{vv}(t) = \frac{1}{3} E(t)^* \int_0^\infty \int_0^\infty \int_{-0.2}^{0.4} \gamma(\tau,\phi,A) e^{-t/\tau} (1 + 2Ae^{-t/\phi}),\ d\tau\ d\phi\ dA \quad (2)$$

$$\text{and } I_{vh}(t) = \frac{1}{3} E(t) * \int_0^\infty \int_0^\infty \int_{-0.2}^{0.4} \gamma(\tau,\phi,A) e^{-t/\tau} (1 - Ae^{-t/\phi}),\ d\tau\ d\phi\ dA \quad (3)$$

where $E(t)$ is the temporal shape of the excitation flash. * denotes a convolution product and $\gamma(\tau, \phi, A)$ represents the number of fluorophores with fluorescence lifetime, τ, rotational correlation time, ϕ, and initial anisotropy, A.

The fluorescence intensity decay is obtained by summing the parallel and perpendicular components: $T(t) = E(t)^* \int_0^\infty \alpha(\tau) \exp(-t/\tau)dt$. $\alpha(\tau)$ is the lifetime distribution given by

$$\alpha(\tau) = \int_0^\infty \int_{-0.2}^{0.4} \gamma(\tau, \phi, A)\ d\phi\ dA \quad (4)$$

In order to ensure that the recovery distribution agrees with the data, the entropy S is maximized:

$$S = \int_0^\infty [\alpha(\tau) - m(\tau) - \alpha(\tau) \log \frac{\alpha(\tau)}{m(\tau)}]\ dt \quad (5)$$

where $m(\tau)$ is the starting lifetime distribution flat in logτ space and $\alpha(\tau)$ is the resulting distribution.[20–25] The entropy S is maximized under the condition that χ^2 is minimized to unity,

$$\chi^2 = \frac{1}{N} \sum_{k=1}^{N} \frac{[I_c(k) - I_0(k)]}{I_0(k)} \quad (6)$$

where N is the number of channels, and $I_c(k)$, and $I_0(k)$ are the calculated and observed number of photons in channel k, respectively.[25]

When fluorescence anisotropy decay is measured, and assuming that there is no correlation between τ and ϕ, $\alpha(\tau)$ and $\beta(\phi)$ are independent. $I_{vv}(t)$ and $I_{vh}(t)$ can be written as

$$I_{vv}(t) = \frac{1}{3} \int_0^\infty \alpha(\tau) e^{-t/\tau} d\tau \int_0^\infty [1 + 2\beta(\phi) e^{-t/\phi}]\ d\phi \quad (7)$$

$$I_{vh}(t) = \frac{1}{3} \int_0^\infty \alpha(\tau) e^{-t/\tau} d\tau \int_0^\infty [1 - \beta(\phi) e^{-t/\phi}]\ d\phi \quad (8)$$

The integrated amplitude $\beta(\phi)$ corresponds to the fundamental anisotropy A_0, and the time dependence of the anisotropy can be described with the integral $A(t) = \int_0^\infty \beta(\phi)e^{-t/\phi}\ d\phi$.[27] In this analysis of the fluorescence and fluorescence anisotropy decay, the entropy of the cross-product $\alpha(\tau) \cdot \beta(\phi)$ is maximized under the constraint of minimum χ^2,

$$S = -\int_0^\infty \alpha(\tau)\ \beta(\phi) \log \frac{\alpha(\tau)\ \beta(\phi)}{m(\tau)} d\tau \quad (9)$$

where $m(\tau)$ is the initial guess of the $\alpha(\tau) \cdot \beta(\phi)$ distribution.

The maximum entropy method can handle Laplace transforms such as those found in pulse fluorometry, without restricting the validity of the solution or suffering from any instabilities. It allows the recovery of the distribution of exponentials describing the decay of the fluorescence (i.e., inverting the Laplace transform), which is, in turn, convolved by the shape of the excitation flash. Also, it can determine the background level and amount of parasitically scattered radiation.[22]

RESULTS

Lifetime Data

Fluorescence intensity, $I(\lambda,t)$ of Trp residues obtained at λ_{ex} equal to 295 nm can be adequately represented by a sum of four exponentials,

$$I(\lambda,t) = 0.7065e^{-t/0.016} + 0.0796e^{-t/0.484} + 0.1285e^{-t/1.6} + 0.0854e^{-t/4.057}$$

where 0.7065, 0.0796, 0.1285, and 0.0854 are the preexponential factors, 0.016 ± 0.007, 0.484 ± 0.113, 1.600 ± 0.442, and 4.057 ± 0.690 are the decay times (ns), and λ the emission wavelength (335 nm). The weighted-average fluorescence lifetime $\bar{\tau}_0$ is equal to 2.912 ns. The value of χ^2 is 1.12.

$$\bar{\tau}_0 = \sum f_i \tau_i \quad \text{and} \quad f_i = \alpha_i \tau_i / \sum \alpha_i \tau_i$$

where α_i are the preexponential terms and τ_i the fluorescence lifetimes.

At 315 nm, the mean fluorescence lifetime was found to be 2.46 ns. This value was used to calculate

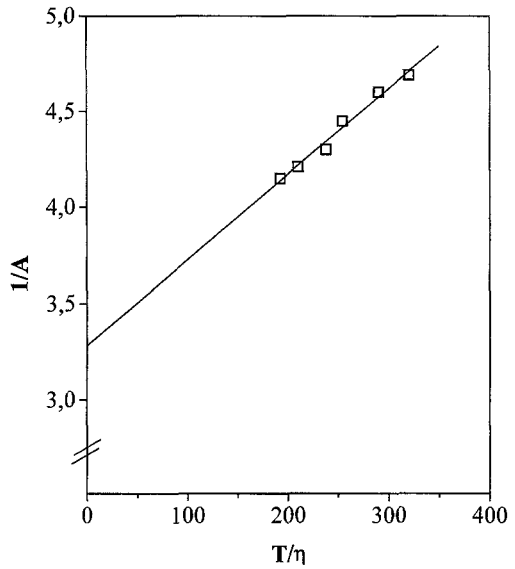

Fig. 1. Steady-state fluorescence anisotropy versus temperature/viscosity ratio for the TNS–LCA complex. Data were obtained by thermal variation of temperature. λ_{ex}, 320 nm; λ_{em}, 430 nm.

the rotational correlation time from the Perrin plot obtained as a function of sucrose (Fig. 3).

The fluorescence intensity decay of TNS in the presence of LCA can be adequately represented by four lifetimes: 10.304 ± 1.864, 4.794 ± 1.206, 1.728 ± 0.407, and 0.414 ± 0.093 ns, with fractional intensities equal to 0.525, 0.355, 0.098, and 0.016, respectively. The excitation and emission wavelengths are 295 and 425 nm, respectively. The lifetime equal to 0.4 ns corresponds to the free TNS in solution[6,26] and the longest lifetimes correspond to the bound TNS. The weighted—average fluorescence lifetime, $\bar{\tau}_0$ = 7.3 ns, was used to calculate the rotational correlation time from the Perrin plot (Fig. 1).

Dynamics of the TNS–LCA Complex

Red-Edge Excitation Shift

Red-edge excitation shift was used as a tool to monitor motions around a fluorophore.[28,29]

Fluorophore molecules and the amino acid residues of their binding sites (in the case of TNS) or of their microenvironment (in the case of Trp residues) have dipoles. The dipole of the excited fluorophore has an orientation different from that of the fluorophore in the ground state. Thus dipole–dipole interactions in the ground state are different from those in the excited state. This new interaction is unstable. The excited fluorophore reorients the dipole of the amino acid residues of the binding site. The dipole reorientation is called a relaxation phenomenon.[30] After relaxation, fluorescence emission occurs. This is the case when relaxation is faster than fluorescence, i.e., the binding site is flexible and the fluorophore can move easily. The emission maximum from a relaxed state does not change with excitation wavelength. When the binding site is rigid, fluorescence emission occurs before relaxation. In this case excitation at the longer wavelength edge of the absorption band photoselects a population of fluorophores that is energetically different from that photoselected when the excitation wavelength is shorter. Thus excitation at the red edge gives a fluorescence spectrum with a maximum located at a higher wavelength than that obtained when excitation is performed at short wavelengths.

The maximum of the fluorescence spectra of bound TNS is a function of the excitation wavelength. At 360 nm, the emission maximum is located at 422 nm. It shifts to higher wavelengths (430 and 440 nm) when the excitation wavelengths are 380 and 400 nm, respectively (data not shown). This is taken as direct evidence that TNS exhibits restricted mobility on LCA, i.e., the fluorophore follows the motion of the protein, suggesting a rotational correlation time equal to that of the protein.

Steady-State Anisotropy as a Function of Temperature

The rotational correlation time (ϕ_p) of a hydrated sphere is obtained from the equation

$$\phi_p = M(\bar{v} + h)\eta/kTN \qquad (10)$$

where M is the protein molecular weight, v = 0.73 cm³/g is the specific volume, h = 0.3 cm³/g is the degree of hydration, and η is the viscosity of the medium. At 20°C, the ϕ_p value of LCA is 22 ns if the protein is spheric.

Fluorescence anisotropy of the TNS–LCA complex (λ_{em} = 430 nm and λ_{ex} = 320 nm) was measured as a function of temperature. The Perrin equation is[30]

$$\frac{1}{A} = \frac{1}{A_0} + \left(\frac{1}{A_0}\right)\frac{RT\bar{\tau}_0}{\eta V} = \frac{1}{A_0} + \left(\frac{1}{A_0}\right)\frac{\bar{\tau}_0}{\phi_F} \qquad (11)$$

where A and A_0 are the anisotropy in the presence and absence of rotational diffusion, respectively, and $\bar{\tau}_0$ = 7.3 ns, η, V, and ϕ_F are the mean fluorescence lifetime, the viscosity, the fluorophore rotational volume, and its rotational correlation time, respectively. Data for the TNS–LCA complex are plotted in Fig. 1.

Table I. Information Obtained from the Various Methods Used to Follow the Global and Local Dynamics of LCA[a]

Method	Fluorophore	
	TNS	Trp residues
Red-edge excitation shift	Microenvironment of the binding site is rigid	Microenvironment of the amino acid is mobile
Perrin method	Rotational correlation time of the protein (thermal variation): ϕ_p = 18.6 ns	Rotational correlation time of the protein and mean rotational time of Trp residues (sucrose variation); ϕ_p = 18.5 ns, ϕ_F = 105 ps
Anisotropy decay	—	Same information as the Perrin plot; ϕ_p = 17 ns, ϕ_F = 351 ps
Quenching resolved emission anisotropy	—	Anisotropies of Trp residues present at the surface and of those buried in the protein core; A_1 = 0.112, A_2 = 0.257

[a]Rotational correlation time of LCA calculated theoretically from Eq. (10) (see text) is 22 ns.

The value of A_0 found from the Perrin plot is 0.305. This value is close to that (0.317) measured at −35°C and indicates that the extrinsic probe has a restricted mobility on LCA. This result is in good agreement with that found in the red-edge excitation shift experiment.

The rotational correlation time ϕ_p (18.6 ns at 20°C), in the same range as that (22 ns) expected for LCA, indicates that the TNS follows the global rotation of the protein (see Table I). Thus, LCA can be considered globular.

Dynamics of the Trp Residues

Red-Edge Excitation Shift

The maximum tryptophan fluorescence (330 nm) of LCA is independent of excitation wavelength (295, 300, and 305 nm). This means that the microenvironments of the Trp residues are not rigid, i.e., the Trp residues exhibit residual motions independent of the global rotation of the protein. In order to separate the global and local rotational correlation times, fluorescence decay anisotropy and/or static fluorescence anisotropy as a function of sucrose could be performed.

Fluorescence Anisotropy Decay

For a fluorophore bound tightly to a protein, the anisotropy decays as a single exponential,

$$A(t) = A_0 e^{-t/\phi_p} \tag{12}$$

where ϕ_p is the rotational correlation time of the protein and A_0 is the limiting anisotropy of the fluorophore at the excitation wavelength.

When the fluorophore has segmental motions, the anisotropy decays rapidly to

$$A_\infty = A_0 (1 - \alpha) \tag{13}$$

However, the anisotropy continues to decay to zero as a result of the overall motion of the macromolecule. Thus time-resolved decay of anisotropy will be analyzed as a sum of exponential decays:[31]

$$A(t) = A_0 \left[\alpha e^{-t/\phi_s} + (1 - \alpha) e^{-t/\phi_p}\right] \tag{14}$$

where A_0 is the limiting anisotropy at $t = 0$ and at the excitation wavelength (λ_{ex}, 295 nm), ϕ_s and ϕ_p are the short and the protein rotational correlation times, respectively, and α and $1 - \alpha$ are the weighting factors for the respective depolarizing processes.

$$\frac{1}{\phi_s} = \frac{1}{\phi_p} + \frac{1}{6\phi_F} \tag{15}$$

Fluorescence anisotropy decay of Trp residues in LCA can be represented by $A(t) = 0.036e^{-t/1.874} + 0.226e^{-t/17}$, where 0.036, 0.226, 1.874, and 17 are $A_0\alpha$, $A_0(1 - \alpha)$, ϕ_s, and ϕ_p, respectively. The steady-state anisotropy A_0 is equal to 0.262 at 295 nm (Fig. 2). The value of χ^2 is 1.082.

ϕ_p = 17 ns, a value close to that (22 ns) calculated theoretically [Eq. (10)] and identical to that (18 ns) obtained with the Perrin plot for bound TNS (Fig. 1).

The presence of the small correlation time (ϕ_s = 1.874 ns) indicates that Trp residues have segmental motions. This is in good agreement with the results obtained by red-edge excitation shift experiments, i.e., Trp residues are mobile with respect to their microenvironment. Two motions contribute to the depolarization process, the local motion of the Trp residues and the global motion of the protein. It is possible to measure the relative importance of the segmental motion (α) of Trp residues

$$A(0)/A_0 = 1 - \alpha \tag{16}$$

and the average angular displacement θ of the fluorophore inside the protein,

$$\cos^2 \phi = 1 - 2\alpha/3 \tag{17}$$

The values of α and θ are 0.1374 and 18°, respectively.

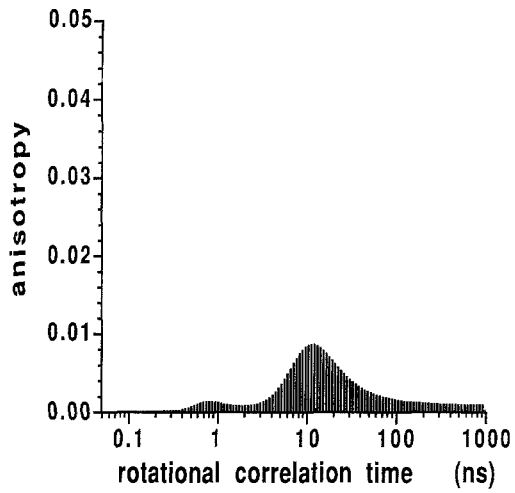

Fig. 2. Correlation–time profile of LCA at 20°C. λ_{ex}, 295 nm; λ_{em}, 335 nm. The value of χ^2 is 1.082. Two values were obtained, 17 and 1.874 ns. The long lifetime represents the global rotation of the protein and the short one indicates the presence of a segmental motion of the Trp residues.

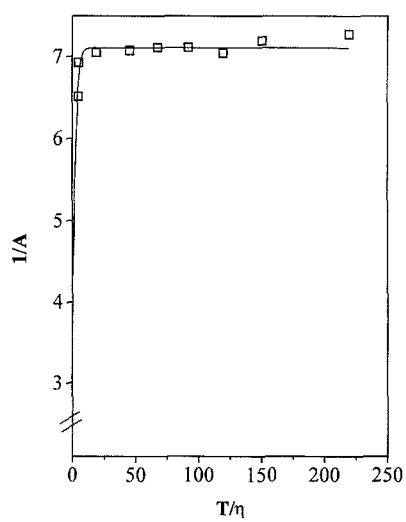

Fig. 3. Steady-state fluorescence anisotropy versus temperature/viscosity ratio for LCA. Data were obtained by variation of sucrose concentration at a constant temperature of 20°C. λ_{ex}, 295 nm; λ_{em}, 315 nm. From the lowest T/η values, we extrapolated to A_0 = 0.262 ($1/A_0$ = 3.817). The value of the rotational correlation time ϕ_F of the residual motion of the Trp residues, 105 ps, was estimated from the extrapolated plot. The value of the rotational correlation time ϕ_p of the global motion of LCA, 18.5 ns, was obtained from the experimental plot at a high T/η.

Equation (15) yields a value of 351 ps for ϕ_F, the segmental motion of the Trp residues. This value is close to that (100 ps) known for a free fluorophore in solution.[6,26,32,33]

Steady-State Anisotropy as a Function of Sucrose

Residual motion of the fluorophore can also be detected by measuring static anisotropy as a function of sucrose concentration. A Perrin plot representation is given (Fig. 3) [Eq. (11)],[30] where $\bar{\tau}_0$ = 2.46 ns for tryptophanyl fluorescence and the value of A_0 is 0.262. Figure 3 shows the Perrin plot of Trp residues of LCA at different concentrations of sucrose (λ_{ex} = 295 nm and λ_{em} = 315 nm). The rotational correlation time of the protein (ϕ_p) calculated at high T/η is 18.5 ns, a value similar to that calculated theoretically (22 ns) and equal to that measured with the fluorescence anisotropy decay (17 ns). Also, the data suggest the existence of a subnanosecond rotational correlation time.

Fluorescence Intensity Quenching with Iodide

LCA contains five Trp residues; three are embedded in the protein matrix and two are at the surface of the protein. The fluorescence may originate from the two classes together or from one class alone. Fluorescence intensity quenching with iodide allows us to obtain the spectra of the two classes of Trp residues. Selective quenching implies that the addition of quencher induces a decrease in the fluorescence observables (intensity, anisotropy, and lifetime) of the accessible class of fluorophore. At a high quencher concentration the remaining observables measured will reflect essentially those of the embedded Trp residues.

Dynamic fluorescence quenching is analyzed by the Stern–Volmer equation:

$$I_0/I = 1 + k_q \bar{\tau}_0 [Q] \qquad (18)$$

where I_0 and I are the fluorescence intensities in the absence and presence of quencher respectively, k_q the bimolecular diffusion constant, $\bar{\tau}_0$ the mean fluorescence lifetime, and $[Q]$ the concentration of iodide added. The Stern–Volmer plot (not shown) at 330 nm shows a downward curvature, indicating selective quenching.[34]

The fraction of the fluorescence intensity that is accessible (f_a) is obtained from the modified Stern–Volmer equation,[35]

$$I_0/\Delta I = 1/f_a + 1/f_a K_{SV} [Q] \qquad (19)$$

where K_{sv} is the Stern–Volmer constant for the fluorescence quenching of the Trp residue(s) by I^- and

$$\Delta I = I_0 - I \qquad (20)$$

Figure 4 shows the plot of the modified Stern–Volmer at 330 nm. In Fig. 5, the fluorescence spectra of LCA (a) (λ_{max} = 330 nm), of the inaccessible Trp residues

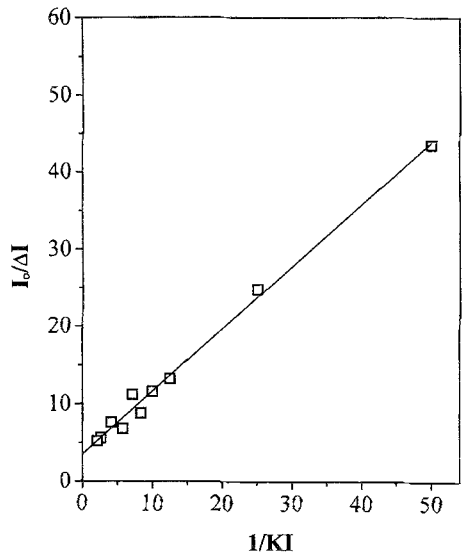

Fig. 4. Modified Stern–Volmer plot of the quenching of LCA Trp residues by iodide ion at 330 nm. λ_{ex}, 295 nm.

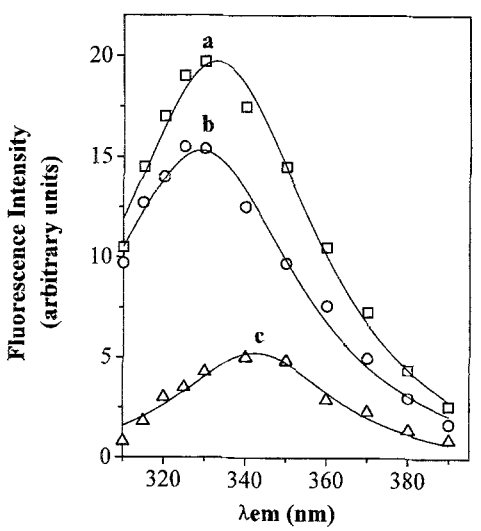

Fig. 5. Fluorescence spectra of LCA (a), of Trp residues exposed to KI (c), and of Trp residues buried in the protein matrix (b). λ_{ex}, 295 nm.

(b) (λ_{max} = 324 nm) obtained by extrapolating to $[I^-] = \infty$, and of the quenched Trp residue(s) (c) obtained by substracting spectrum (b) from spectrum (a), are displayed. The emission maximum of the accessible Trp residues is located at 345 nm, a characteristic of an emission from Trp residues near the surface of the protein. Figure 5 indicates clearly that both classes of Trp residues contribute to the fluorescence spectrum of LCA.

Quenching Resolved Emission Anisotropy

Red-edge excitation shift, fluorescence anisotropy decay measurements, and Perrin plot as a function of sucrose reveal that Trp residues in LCA have independent motions. The results obtained contain contribution from the five residues. In order to study the dynamic behavior of each class of tryptophanyl residues, steady-state measurements of emission anisotropy under conditions of selective quenching were performed. This method consists of quenching fluorescence parameters of the Trp residue on the protein surface, thus, the remaining fluorescence signal will reflect that of buried Trp residues, i.e., Trp residues not accessible to the quencher.[12] By following anisotropy and intensity variation as a function of quencher concentration, it will be possible to obtain information on the motion of each class of the Trp residues.

In general, when anisotropy varies as a function of quencher concentration, the Perrin plot can be written as

$$\frac{1}{A} = \frac{1}{A_0} + \frac{\bar{\tau}_0 I/I_0}{\phi_F A_0} \tag{21}$$

where I and I_0 are the fluorescence intensities in the presence and absence of collisional quencher. When the fluorescence lifetime $\bar{\tau}_0$ and intensity I_0 decrease by collisional quenching, the anisotropy $A(\tau)$ increases and tends to the limiting anisotropy A_0. However, the existence of the residual motions will lead to an extrapolated anisotropy $A(0)$ different from A_0 and to a rotational correlation time lower than ϕ_p. Thus plotting $1/A$ vs $I\,\bar{\tau}_0/I_0$ will yield information concerning the motion of the fluorophore.

Information obtained from Eq. (21) requires that the quencher diffuses in all parts of the protein and collides with the Trp residues, inducing a decrease in the fluorescence intensity and lifetime. However, fluorescence quenching of all Trp residues is not necessarily identical because of different motions that can exist in the microenvironment of the different classes of Trp residues. Thus using a nonselective quencher such as oxygen will yield information on the mean motion of all Trp residues in the protein.[36] In order to evaluate the contribution of each class of Trp residues to the global motion, selective quenching is necessary.

Measurements of the emission anisotropy A as a function of added collisional quencher are made with the steady fluorescence intensity, which integrates the different weighted fluorescence lifetimes.

Anisotropy of each class of residue can be determined in the following way: at $[Q] = 0$ (at I_0), the anisotropy A measured is the weighted average,

$$A = f_a A_1 + f_b A_2 \quad (22)$$

At $[Q] = \infty$, the remaining fluorescence intensity and anisotropy are I_2 and A_2, that of the inaccessible class of residues. The ratio

$$I_2/I_0 = f_b \quad (23)$$

the fractional intensity of the inaccessible residues at $[Q] = 0$. Knowing A_2, f_a, and f_b, one can calculate A_1 from the value of A in the absence of quencher.

All quenching resolved emission anisotropy experiments were measured at an excitation wavelength equal to 300 nm to provide a high limiting anisotropy A_0 and to avoid excitation of tyrosine residues. Also, by exciting at the red edge of the absorption spectrum, energy transfer between Trp residues is eliminated as a possible depolarizing process.[37] However, excitation at the red edge of absorption spectra decreases the amount of light absorbed by the fluorophore and increases the possibility of contributions from scattered light. For this reason, we corrected for the Raman effect of the buffer. In all instances, Raman effects did not account for more than 5% of the total signal.

We performed our experiments at an emission wavelength of 315 nm. At this wavelength, the fluorophore present at the surface of the protein contributes about 12% ($f_a = 0.12$) of the total fluorescence (Fig. 5).

Quenching resolved emission anisotropy plot of A vs I/I_0 (not shown) yields a value of A_2 equal to 0.257 and that of A_1 equal to 0.112. The value of A_2 indicates that the Trp residues embedded in the protein core still have motions if we consider that the limiting anisotropy known for Trp residues at an excitation wavelength of 300 nm is 0.3. The low value of A_1 indicates that the Trp residues present at the surface of the protein have residual motions and may also indicate that the residues on the surface have a shorter average fluorescence lifetime.

DISCUSSION

Structures but not internal dynamics of many lectins and lectin–carbohydrate complexes have been determined.[38–44] *Lens culinaris* agglutinin and concavalin A from *Canavalia ensiformis*, a lectin with a high affinity for α-mannose, show the same secondary structure[4] as if the folding of the two polypeptides has been well conserved during evolution.

Homologies in the amino acid sequences were found between the two lectins, especially in the sequence of amino acids, which plays an important role in the architecture of a hydrophobic cavity, surrounded mainly by hydrophobic residues.[45–47] This may explain why it is very difficult to dissolve LCA in a polar solvent. The saccharide binding site on concavalin A was found to be 20 Å away from the hydrophobic cavity,[48,49] and X-ray diffraction studies on LCA indicated that the carbohydrate binding site is flexible.[5]

Red-edge excitation shift experiments and the Perrin plot of the TNS–LCA complex indicate that local motions around TNS molecules are nonexistent. Thus the hydrophobic site of LCA is rigid.

LCA recognizes α-L-fucose. The affinity between LCA and lactotransferrin, a protein that contains α-L-fucose as a side chain, is high.[50] The interaction occurs mainly between amino acids of the LCA and the fucose. Addition of lactotransferrin to a LCA-TNS complex does not induce any decrease in the fluorescence intensity of TNS (not shown), as would be expected for competitive binding.[51] Thus, the TNS binding site on LCA is different from the carbohydrate binding site.

The red-edge excitation shift (18 nm) observed for the TNS–LCA complex is in good agreement with the results observed when the fluorophore is bound tightly to other proteins, such as apomyoglobin,[52] melittin,[53] and α_1-acid glycoprotein (orosomucoid).[10,11] In fact, an important red-edge excitation shift (8, 11.5, and 15 nm, respectively) was observed when the excitation wavelength was changed from 360 to 400 nm.

The fluorescence maximum of TNS bound to LCA is located at 422 nm (λ_{ex}, 320 and 360 nm). This wavelength is close to that observed for TNS dissolved in solvents of low polarity such as butanol (420 nm) and ethanol (425 nm).[11] However, since a red-edge excitation shift does not occur in these solvents,[54] the spectral properties of TNS in liquid isotropic solvents and when bound to a protein are not equivalent. In a solvent, the fluorescence emission of TNS will depend mainly on the hydrophobicity of the medium. On a protein, the fluorescence may occur from a nonrelaxed and a polar state, from a relaxed and a nonpolar state, or from a nonrelaxed and a nonpolar state. For example, TNS on orosomucoid (λ^{max} = 425 nm) is in a polar and a nonrelaxed area (the surface of the protein),[10,11] and TNS on apomyoglobin is in a nonpolar and nonrelaxed region, the heme pocket.[52] Our results indicate that, on LCA, TNS is bound to a rigid and hydrophobic site.

The rotational correlation time (18.6 ns) found for the TNS–LCA complex with the Perrin plot (Fig. 1) and the extrapolated anisotropy (0.305) confirm the red-edge excitation shift experiment, i.e., the TNS binding site is rigid on the protein.

The protein fluorescence spectrum with a maximum at 324 nm (Fig. 5b) originates from the three buried Trp residues, while that with a maximum at 345 nm (Fig. 5c) originates from the two Trp residues near the protein surface. The maximum of the fluorescence spectrum of LCA is located at 330 nm (Fig. 5a), with an intensity close to that obtained for the buried Trp residues. Thus the buried Trp residues are responsible for the major component of LCA's fluorescence.

The protein fluorescence is described by four lifetimes. Since one Trp residue may have multiple fluorescence lifetimes, we did not attempt in this work to assign the fluorescence lifetimes to any particular Trp residues. The short fluorescence lifetime (0.016 ns) is probably due to the existence of a resonance–energy homotransfer between the Trp residues or scattered light. This energy transfer can be put into evidence by measuring the anisotropy decay in the absence of rotational diffusion, i.e., in glycerol solution and at a low temperature (−40°C).[20] In our work we did not study this possible energy homotransfer.

The absence of red-edge excitation shift for Trp residues agrees with the interpretation that emission occurs from a relaxed state, i.e., motions around Trp residues do exist.

The mean local motion of Trp residues was characterized with the time-resolved decay of anisotropy and with the static polarization as a function of sucrose. The short rotational correlation time (351 ps) calculated with the time-resolved decay of anisotropy (Fig. 2) may have contributions from all five Trp residues. The long rotational correlation time (17 ns) found for LCA from the fluorescence anisotropy decay experiment is of the same order as that (22 ns) expected for a globular protein of molecular weight 52,570.

Quenching resolved emission anisotropy (QREA) experiments reveal that this local motion concerns both classes of Trp residues but indicate that the Trp residues embedded in the protein matrix are more restricted by the surrounding amino acid residues than those of the protein surface. Loris *et al.*[5] found that the lectin dimers are packed in a very loose structure and the amino acid residues facing the solvent (i.e., present at the surface of the protein) are flexible. Our results obtained with TNS show the existence of a rigid and a hydrophobic pocket near the surface of the protein. This result is in good agreement with that found for concavalin A. Thus, LCA has at least three dynamic domains: a completely rigid core, the binding site of TNS; a second partially rigid core; and a third surface domain that has free motion. The fact that amino acid residues of the surface are much more mobile than those present in the core of the protein is in good agreement with the results obtained on other proteins such as lysozyme,[12] LADH,[55] and orosomucoid.[56]

In theory, QREA seems to be very simple. However, the measurements are difficult when using a selective quencher and when there is a small change in the steady-state anisotropy values. The reason for this small variation is that only a small fraction of the total fluorescence intensity is quenched, thus limiting the observed change in the steady-state anisotropy. This is not the case when a nonselective quencher such as oxygen is used. For example, fluorescence quenching of Trp residues in LADH by oxygen induces an increase in the steady-state anisotropy from 0.077 to 0.125 at 24°C.[57] Also, it was found that oxygen efficiently quenches the fluorescence of porphyrin–myoglobin. This quenching induces an increase in the steady-state anisotropy from 0.037 at a 0.218 m*M* oxygen concentration to 0.0875 in the presence of 88 m*M* oxygen.[58]

As with concavalin A, LCA binds to various structures via hydrophobic interactions independently of the saccharide-binding activity. We suggest that the lectin acts as a bipolar component between the hydrophobic membrane and the hydrophilic carbohydrate. This may explain the multiple interactions of the exogeneous carbohydrate with cell membranes.

ACKNOWLEDGMENTS

The author wish to thank Professor Henry Debray (Laboratoire de Chimie-biologique, University of Lille 1) for providing LCA, Drs. Jacques Gallay and Michel Vincent (LURE, Orsay) for their help in the lifetime and anisotropy decay measurements, Dr. R. Loris (Institute for Molecular Biology, Sint-Genesius Rode, Belgium) for the information concerning the accessibility of Trp residues of LCA to the protein surface, and the referee for his constructive criticism.

REFERENCES

1. I. E. Liener (1976) *Annu. Rev. Plant Physiol.* **27**, 291–319.
2. N. Sharon (1977) *Sci. Am.* **236**, 108–119.
3. A. Foriers, R. De Nève, L. Kanarek, and A. D. Strosberg (1978) *Proc. Natl. Acad. Sci. USA* **75**, 1136–1139.
4. A. Foriers, E. Lebrun, R. Van Rajenbusch, R. De Nève, and A. D. Strosberg (1981) *J. Biol. Chem.* **256**, 5550–5560.
5. R. Loris, J. Steyaert, D. Maes, J. Lisgarten, R. Pickersgill, and L. Wyns (1993) *Biochemistry* **32**, 8772–8781.
6. J. Oton, E. Bucci, R. F. Steiner, C. Fronticelli, D. Franchi, J. Montemarano, and A. Martinez (1981) *J. Biol. Chem.* **256**, 7248–7256.

7. J. R. Lakowicz and S. Keating-Nakamoto (1984) *Biochemistry* **23**, 3013–3021.
8. Ch. Mohan-Rao, S. Chenchal Rao, and P. Bheema Rao (1989) *Photochem. Photobiol.* **50**, 399–402.
9. Z. Wasylewski, H. Koloczek, A. Wasniowska, and A. Slizowska (1992) *Eur. J. Biochem.* **206**, 235–242.
10. J. Albani (1992) *Biophys. Chem.* **44**, 129–137.
11. J. Albani (1994) *J. Biochem.* **116**, 625–630.
12. M. Eftink (1983) *Biophys. J.* **43**, 323–334.
13. D. D. Roberts and I. J. Goldstein (1983) *Arch. Biochem. Biophys.* **224**, 479–484.
14. S. Toyoshima, T. Osawa, and A. Tonomura (1970) *Biochim. Biophys. Acta* **221**, 514–521.
15. I. K. Howard, H. G. Sage, M. D. Stein, M. N. Young, M. A. Leon, and D. F. Dyckes (1971) *J. Biol. Chem.* **246**, 1590–1595.
16. J. Hoebeke, A. Foriers, A. B. Schreiber, and A. D. Strosberg (1978) *Biochemistry* **17**, 5000–5005.
17. W. O. McClure and G. M. Edelman (1966) *Biochemistry* **5**, 1908–1918.
18. J. R. Lakowicz (1983) in *Principles of Fluorescence Spectroscopy*, Plenum, New York, p. 44.
19. O. P. Kuipers, M. Vincent, J. C. Brochon, H. M. Verheij, G. H. De Hass, and J. Gallay (1991) *Biochemistry* **30**, 8771–8785.
20. M. Vincent, I. M. Li de la Sierra, M. N. Berberan-Santos, A. Diaz, M. Diaz, G. Padron, and J. Gallay (1992) *Eur. J. Biochem.* **210**, 953–961.
21. M. Vincent, A. M. Deveer, G. H. De Hass, H. M. Verheu, and J. Gallay (1993) *Eur. J. Biochem.* **215**, 531–539.
22. A. K. Livesey and J.-C. Brochon (1987) *Biophys. J.* **52**, 693–706.
23. P. Blandin, F. Mérola, J.-C. Brochon, O. Trémeau, and A. Ménez (1994). *Biochemistry* **33**, 2610–2619.
24. J. Sopkova, J. Gallay, M. Vincent, P. Pancoska, and A. Lewit-Bentley (1994) *Biochemistry* **33**, 4490–4499.
25. R. Leenders, A. Van Hoek, M. Van Iersel, C. Veeger, and A. J. W. G. Visser (1993) *Eur. J. Biochem.* **218**, 977–984.
26. B. J. M. Thevenin, N. Periasamy, S. B. Shohet, and A. S. Verkman (1994) *Proc. Natl. Acad. Sci. USA* **91**, 1741–1745.
27. E. H. W. Pap, J. J. ter Horst, A. Van Hoek, and A. J. W. G. Visser (1994) . *Biophys. Chem.* **48**, 337–351.
28. A. P. Demchenko and N. V. Shcherbatska (1985) *Biophys. Chem.* **22**, 131–143.
29. S. Murkherjee and A. Chattopadhyay (1994) *Biochemistry* **33**, 5089–5097.
30. G. Weber (1952) *Biochem. J.* **51**, 145–155.
31. Y. Gottlieb and Ph. Wahl (1963) *J. Chim. Phys.* **60**, 849–856.
32. P. M. Mulqueen and M. J. Kronman (1982) *Arch. Biochem. Biophys.* **215**, 28–39.
33. J. R. Albani, R. Vos, K. Villaert, and Y. Engelborghs (1995) *Photochem. Photobiol.* **62**, 30–34.
34. M. R. Eftink and C. A. Ghiron (1976) *Biochemistry* **15**, 672–680.
35. S. S. Lehrer (1971) *Biochemistry* **10**, 3254–3263.
36. J. R. Lakowicz and G. Weber (1973) *Biochemistry* **12**, 4171–4179.
37. G. Weber and M. Shinitzky (1970) *Proc Natl Acad Sci USA* **65**, 823–830.
38. J. W. Becker, G. N. Reeke, J. L. Wang, B. A. Cunningham, and G. M. Edelman (1975) *J. Biol. Chem.* **250**, 1513–1514.
39. K. D. Hardman, R. C. Agarwal, and M. J. Feisner (1984) *J. Mol. Biol.* **157**, 69–89.
40. N. R. Reeke and J. W. Becker (1986) *Science* **234**, 1108–1111.
41. H. Einspahr, H. E. Parks, K. Sugana, E. Subramanian, and F. L. Suddath (1986) *J. Biol. Chem.* **261**, 16518–16527.
42. Y. Bourne, C. Abergel, C. Cambillau, M. Frey, P. Rougé, and J. C. Fontecilla-Camps (1990) *J. Mol. Biol.* **214**, 571–584.
43. Y. Bourne, A. Roussel, M. Frey, P. Rougé, J. C. Frontecilla-Camps, and C. Cambillau (1990) *Proteins Struct. Funct. Genet.* **8**, 365–376.
44. B. Shaanan, H. Lis, and N. Sharon (1991) *Science* **254**, 862–866.
45. A. Foriers, C. Wunilmart, N. Sharon, and A. D. Strosberg (1977) *Biochem. Biophys. Res. Commun.* **75**, 980–986.
46. E. Van Driessche, A. Foriers, A. D. Strosberg, and L. Kanarck (1976) *FEBS Lett.* **71**, 220–222.
47. A. Foriers, E. Van Driessche, R. De Nève, L. Kanareck, and A. D. Strosberg (1977) *FEBS Lett.* **75**, 237–240.
48. J. W. Becker, G. N. Reeke, Jr., B. A. Cunningham, and G. M. Edelman (1976) *Nature* **259**, 406–409.
49. K. D. Hardman and C. F. Ainsworth (1976) *Biochemistry* **15**, 1120–1128.
50. H. Debray, D. Decout, G. Strecker, G. Spik, and J. Montreuil (1981) *Eur. J. Biochem.* **117**, 41–55.
51. J. Albani (1985) *Arch. Biochem. Biophys.* **243**, 292–297.
52. A. Gafni, R. P. De Toma, R. E. Manrow, and L. Brand (1977) *Biophys. J.* **17**, 155–168.
53. A. P. Demchenko (1985) *FEBS Lett.* **182**, 99–102.
54. A. P. Demchenko (1982) *Biophys. Chem.* **15**, 101–109.
55. J. B. A. Ross, J. Schmidt, and L. Brand (1981) *Biochemistry* **20**, 4369–4377.
56. J. Albani (1996) *Biochim. Biophys. Acta* **129**, 215–220.
57. J. R. Lakowicz, B. P. Maliwal, H. Cherek, and A. Balter (1983) *Biochemistry* **22**, 1741–1752.
58. J. Albani and B. Alpert (1986) *Chem. Phys. Lett.* **131**, 147–152.